

Model independent tests of the Kerr bound with extreme mass ratio inspirals

Gabriel Andres Piovano¹, Andrea Maselli¹, Paolo Pani¹

¹ *Dipartimento di Fisica, “Sapienza” Universit di Roma & Sezione INFN Roma1, Piazzale Aldo Moro 5, 00185, Roma, Italy*

An outstanding prediction of general relativity is the fact that the angular momentum S of an isolated black hole with mass μ is limited by the Kerr bound, $S \leq G\mu^2/c$. Testing this cornerstone is challenging due to the difficulty in modelling spinning compact objects that violate this bound. We argue that precise, model-independent tests can be achieved by measuring gravitational waves from an extreme mass ratio inspiral around a supermassive object, one of the main targets of the future LISA mission. In the extreme mass ratio limit, the dynamics of the small compact object depends only on its multipole moments, which are free parameters. At variance with the comparable-mass case, accurate waveforms are valid also when the spin of the small object greatly exceeds the Kerr bound. By computing the orbital dephasing and the gravitational-wave signal emitted by a spinning point particle in circular, nonprecessing, equatorial motion around a Kerr black hole, we estimate that LISA will be able to measure the spin of the small compact object at the level of 10%. Together with mass measurements, this will allow for theory-agnostic, unprecedented constraints on string-theory inspired objects such as “superspinars”, almost in their entire parameter space.

Introduction. The dawn of black-hole (BH) physics can be arguably traced back to the seminal work by Penrose [1, 2], Wheeler [3], Hawking [4], Bekenstein [5, 6], Carter [7, 8], and many others during the first “golden age” of general relativity (GR) in the 1970s. Since then, the field has evolved dramatically and several theoretical predictions have been experimentally confirmed to exquisite precision [9–11]. Nonetheless, some basic relativistic effects associated with BHs remain elusive and have not been yet tested directly.

Arguably the most striking one is the fact that, within GR, a BH with mass μ can spin only below a critical value¹ of the angular momentum S ,

$$|S| \leq S_{\max} \equiv \frac{G\mu^2}{c} \approx 2 \times 10^{44} \left(\frac{\mu}{15M_{\odot}} \right)^2 \text{ kg m}^2/\text{s}, \quad (1)$$

above which a naked singularity would appear. Indeed, the unique stationary solution to GR in vacuum is the Kerr metric, which is regular outside an event horizon only if the above “Kerr bound” is fulfilled. Therefore, any evidence of $|S| > S_{\max}$ in a compact object would imply either the presence of matter fields (e.g., compact stars can theoretical exceed the Kerr bound) or a departure from GR.

High-energy modifications to GR such as string theories can resolve curvature singularities, making the Kerr bound superfluous. Indeed, in these theories compact objects violating the bound (1) – so-called *superspinars* – arise generically [13]. A representative example is the large class of regular microstate geometries in supergravity theories (e.g. [14–18]). These solutions have the same

asymptotic metric of a Kerr BH, and their deviations in the near-horizon region are suppressed by powers of $M_P/\mu \ll 1$, where M_P is the Planck mass. Therefore, besides the possible violation of the Kerr bound and its consequences (e.g. for the accretion efficiency of compact objects [13]), these solutions are practically indistinguishable from a BH (see Ref. [19] for a review). In this context, testing the bound (1) provides a *model-independent* way to test GR and high-energy extensions thereof.

However, testing the Kerr bound is very challenging [19–23]. The standard route is to interpret observations in various contexts *assuming* the Kerr metric and look for inconsistencies in explaining the data. This strategy is not optimal as one would wish to compare the Kerr case with some alternative and perform Bayesian model selection. The latter option is however hampered by the fact that the geometry of spinning BHs beyond GR [21] – or of spinning extreme compact objects without a horizon [19] (such as boson stars) – is known only perturbatively or numerically [24–33]. Furthermore, regardless of the technical difficulties, any analysis based on a specific model or theory would be limited to that specific case, whereas performing a model-independent test of the Kerr bound (1) would be much more profitable. In this respect, it is challenging to devise a test which is at the same time robust and sufficiently general. For example, one could try to measure the spins of the components of a comparable-mass binary using inspiral-merger-ringdown templates [34]; however, the latter *assume* the two objects are Kerr BHs. Likewise, a generic post-Newtonian [35] parametrization of the inspiral suffers from the fact that higher-order spin corrections enter at high post-Newtonian order, making the waveform of highly-spinning binaries less precise near coalescence. Furthermore, the post-Newtonian gravitational-wave (GW) phase contains terms that explicitly assume the validity of the Kerr bound (e.g. the tidal heating term [36–38]), so it is impossible to include violations

¹ The normalized bound, $S_{\max}/\mu^2 = 1$ (in $G = c = 1$ units henceforth adopted [12]), is very modest: a solid ball of mass 1 kg and radius 10 cm making one revolution per second has $S/\mu^2 \sim 10^{17}$. On the other hand, a millisecond pulsar has $S/\mu^2 \approx 0.3$ (assuming standard values $\mu \approx 1.4M_{\odot}$ and moment of inertia $I \approx 10^{45} \text{ g cm}^2$).

consistently.

In this letter and in a companion technical paper [39], we show that many of the above issues can be resolved with tests based on extreme mass ratio inspirals (EMRIs), which are also model independent to a large extent. EMRIs are one of the main targets of the future space-based Laser Interferometer Space Antenna (LISA) [40] and of evolved concepts thereof [41]. Owing to the large number of GW cycles, EMRI signals detectable by LISA can be used to extract the binary parameters with exquisite accuracy [42], and to perform unique tests of fundamental physics [42–52] (see [23, 53] for some recent reviews).

Remarkably, EMRIs allow to devise tests which do not require any assumption on the specific properties of the secondary other than specifying its multipole moments. This is a great advantage to study generic (and arguably vague) proposals such as the superspinar one.

Setup. In an EMRI a small, stellar-size, compact object (dubbed as secondary) of mass μ orbits around a supermassive object (dubbed as primary) of mass $M \sim (10^6 - 10^9)M_\odot$; the typical mass ratio of the system is $q = \mu/M \in (10^{-7} - 10^{-4})$ and therefore allows for a small- q expansion of Einstein’s equations. To the leading order in q , the dynamics is described by a point particle of mass μ in motion around the primary. The orbits evolve quasi-adiabatically through a sequence of geodesics due to energy and angular momentum loss carried away by GWs [54, 55]. To higher order in a small- q expansion, the dynamics can still be described by a point particle endowed with a series of multipole moments. The post-adiabatic corrections depend on self-force effects [55] and also on the intrinsic angular momentum S of the secondary, which is the main target of our investigation. It is convenient to introduce the dimensionless quantity

$$\sigma \equiv \frac{S}{\mu M} = \chi q, \quad (2)$$

where $\chi \equiv S/\mu^2$ is the reduced spin of the secondary. Owing to the mass ratio dependence, for an EMRI $|\sigma| \ll 1$ even when χ is very large, since it is sufficient that $|\chi| \ll 1/q \sim (10^4 - 10^7)$. Therefore, it is possible to linearize the dynamics to $\mathcal{O}(\sigma)$ even when χ is large. This is an enormous advantage relative to other cases, e.g. post-Newtonian waveforms of comparable mass binaries. Thus, in order to test the Kerr bound (1) we can study the EMRI evolution in which the secondary is assumed to be either a Kerr BH, which fulfills the constraint $|\chi| \leq 1$, or an extreme compact object [19] that can violate such a bound, i.e. $|\chi| > 1$.

High-curvature corrections for the primary are negligible compared to the secondary. For concreteness, let us consider an effective field theory described by the Einstein-Hilbert Lagrangian with higher-order curvature terms [21] in the schematic form

$$\mathcal{L} = R + \beta \mathcal{R}^n + \dots, \quad (3)$$

where $n > 1$, R is the Ricci scalar, \mathcal{R} is some curvature scalar operator, and β is a coupling constant with dimensions of $(\text{mass})^{2n-2}$. It is easy to see that the corrections to the primary are suppressed by a factor $1/q^n \gg 1$ or higher [39]. Therefore, to an excellent approximation we can assume that the background spacetime (i.e. the primary) is described by the Kerr metric with mass M and angular momentum $J \equiv \hat{a}M^2$ satisfying the Kerr bound, i.e. $|\hat{a}| \leq 1$.

The dynamics of the spinning point particle on the Kerr background can be obtained through the covariant conservation of the energy-momentum tensor leading to the Mathisson-Papapetrou-Dixon equations of motion [56–63]. We integrate such equations supplied by the Tulczyjew-Dixon condition, $S^{\mu\nu}p_\nu = 0$, between the spin tensor $S^{\mu\nu}$ and the body 4-momentum p^μ [64]. This constraint fixes the center of mass reference frame, and guarantees that the squared mass $\mu^2 = -p_\mu p^\mu$ and spin magnitude $S^2 = \frac{1}{2}S_{\mu\nu}S^{\mu\nu}$ are conserved during the orbital evolution.

During its motion the secondary acts as a perturbation of the background spacetime. Within GR, GW emission from the binary can be computed using the Teukolsky formalism [65–67].

$$\Delta^2 \frac{d}{dr} \left(\frac{1}{\Delta} \frac{dR_{\ell m \omega}}{dr} \right) - V_{\ell m \omega}(r) R_{\ell m \omega} = \mathcal{T}_{\ell m \omega}(r), \quad (4)$$

for any integer $\ell \geq 2$ and $|m| \leq \ell$. The effective potential $V_{\ell m \omega}(r)$ is given in Ref. [55], whereas the source term $\mathcal{T}_{\ell m \omega}(r)$ depends on the stress-energy tensor of the secondary. The latter depends explicitly on the spin σ in two ways: directly, since the spin of the secondary affects the energy content of the source, and indirectly through the trajectory of the secondary, which is affected by spin-angular momentum couplings. The final expression is cumbersome and derived in detail in Ref. [39].

We shall neglect extra radiation channels and consider only the standard GW emission in GR. The motivation for this choice is twofold: (i) superspinars can also arise within GR in the presence of exotic matter fields, in which case our analysis is exact; (ii) in case of higher-curvature corrections to GR as in Eq. (3) the ordinary GW emission remains unchanged in the EMRI limit, but there might be further dissipation channels (e.g. dipolar radiation) in case the secondary is charged under a massless field [68]. However, in the context of supergravity and string theories, putative extra degrees of freedom are expected to be extremely heavy and therefore do not propagate at the frequency of an EMRI. Thus, corrections to the dissipative sector are also negligible. At any rate, extra putative dissipative channels (e.g. due to massless degrees of freedom) can be straightforwardly accommodated within our framework.

GW flux. We numerically integrate Eq. (4) using a standard Green function approach [39], which allows us to compute the energy fluxes down to horizon, \dot{E}_{GW}^- , and

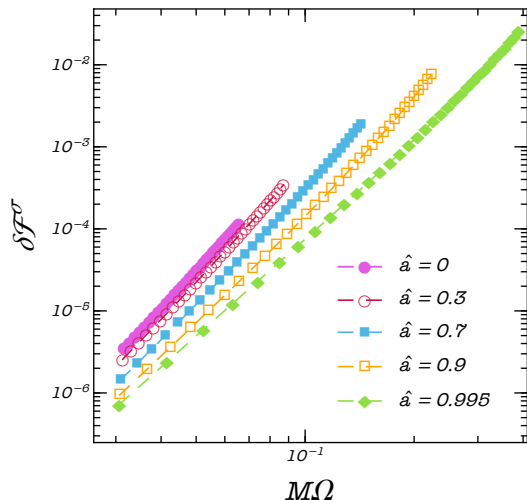


FIG. 1. The spin-correction coefficient $\delta\dot{E}_{\text{GW}}^\sigma$ [see Eq. (6)] as a function of the orbital frequency (up to the ISCO) for different values of the spin $\hat{a} \equiv J/M^2$ of the primary.

at infinity, \dot{E}_{GW}^+ . The impact of the spin of the secondary on the GW fluxes has been studied in Refs. [69–78]. A detailed analysis of the fluxes and a comparison with previous work [72, 76, 77, 79, 80] is presented in Ref. [39].

In the EMRI limit the radiation-reaction time scale is much longer than the orbital period. We can therefore assume that the inspiral is quasi-adiabatic. Under this approximation the system evolves as the change in the binding energy \dot{E}_{orb} is balanced by the total GW flux at infinity and at the horizon,

$$-\dot{E}_{\text{orb}} = \dot{E}_{\text{GW}} = \dot{E}_{\text{GW}}^+ + \dot{E}_{\text{GW}}^- . \quad (5)$$

The flux balance law is valid also when the spin of the secondary is taken into account [76]. Assuming that the secondary spin remains constant during the evolution, angular-momentum fluxes are directly related to the energy ones [39, 69, 81]. All fluxes are decomposed in multipole modes [$\ell = 2, 3, \dots$ in Eq. (4)]. In our calculations we sum the multipole contributions up to $\ell = 20$; truncation errors are 0.05% in the most extreme cases, i.e. $\hat{a} = 0.995$ at the innermost stable circular orbit (ISCO), and typically much smaller [39].

Furthermore, in the adiabatic approximation a two-time scale analysis shows that during the EMRI evolution the masses and spins of the binary can be neglected to leading order [82]. Likewise, the evolution of the spin of the secondary – which introduce dissipative self-torque [76] – is subdominant with respect to the effects discussed here [39].

Results. In the $|\sigma| \ll 1$ limit, the GW flux can be expanded at fixed orbital frequency Ω as

$$\dot{E}_{\text{GW}} = q^2 \left(\dot{E}_{\text{GW}}^0 + \sigma \delta\dot{E}_{\text{GW}}^\sigma + \mathcal{O}(\sigma^2) \right) , \quad (6)$$

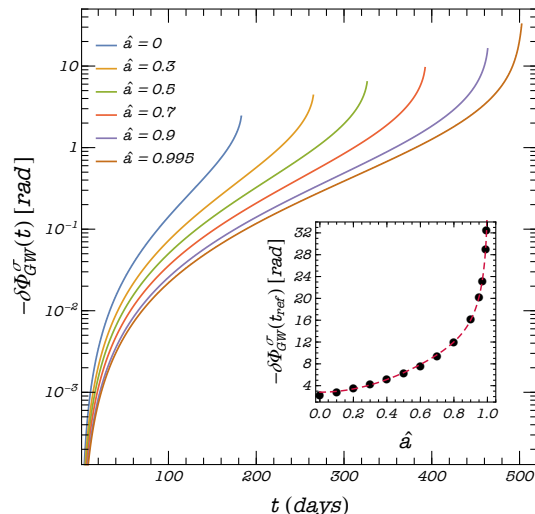


FIG. 2. Spin correction, $\delta\Phi_{\text{GW}}^\sigma(t)$, to the instantaneous GW phase [cf. Eq. (8)] as a function of time up to the ISCO for different values of the spin \hat{a} of the primary. The inset shows the spin correction, $\delta\Phi_{\text{GW}}^\sigma(t_{\text{ref}})$, to the total accumulated phase. The dashed colored curve shows the fit (9). We assumed $\mu = 30M_\odot$ and $M = 10^6M_\odot$ as reference values. Note that in general $\delta\Phi_{\text{GW}}^\sigma(t_{\text{ref}}) < 0$, i.e. when $\chi > 0$ the inspiral lasts longer. Data are publicly available [84].

where we have factored out an overall mass-ratio dependence, \dot{E}_{GW}^0 is the (normalized) flux for a nonspinning secondary, whereas $\delta\dot{E}_{\text{GW}}^\sigma$ is the (normalized) spin contribution of the secondary. As anticipated, the latter is suppressed by a factor of $\mathcal{O}(q)$ relative to the leading-order term. It therefore enters at the same order as the leading-order conservative part and the second-order dissipative part of the self-force [55, 83]. In Fig. 1 we show $\delta\dot{E}_{\text{GW}}^\sigma$ as a function of the orbital frequency, $\Omega = \Omega(r)$. As expected, the correction becomes stronger when the orbit approaches the ISCO (i.e. for higher frequencies) and when the primary is rapidly spinning.

With the fluxes \dot{E}_{GW} at hand, it is possible to calculate the evolution of the orbital frequency $r(t)$ and phase $\Phi(t)$ due to radiation losses. In the adiabatic approximation,

$$\frac{dr}{dt} = -\dot{E}_{\text{GW}}(r) \left(\frac{dE}{dr} \right)^{-1} , \quad \frac{d\Phi}{dt} = \Omega(r) , \quad (7)$$

where the particle energy E and the angular velocity Ω are analytical (albeit cumbersome) functions of (r, \hat{a}, σ) [39, 85, 86]. The flux $\dot{E}_{\text{GW}}(r)$ is obtained by interpolating the calculated fluxes in the range $r \in (r_{\text{start}}, r_{\text{ISCO}})$. The starting point r_{start} is chosen such that the initial orbital frequency is the same as in the case of a nonspinning particle at the reference value $r = 10.1M$.

By integrating the system (7) we can obtain the *instantaneous* orbital phase, which is related to the GW phase of the dominant mode by $\Phi_{\text{GW}} = 2\Phi$. The latter

can be schematically written as

$$\Phi_{\text{GW}}(t) = \frac{1}{q} (\Phi_{\text{GW}}^0(t) + \sigma \delta\Phi_{\text{GW}}^\sigma(t) + \mathcal{O}(\sigma^2)), \quad (8)$$

where $\Phi_{\text{GW}}^0(t)$ is the (normalized) phase for a nonspinning secondary, $\delta\Phi_{\text{GW}}^\sigma(t)$ is the (normalized) spin correction, and we have factored out an overall q^{-1} dependence. As expected, the spin correction is suppressed by a factor of $\mathcal{O}(q)$ and is therefore independent of q to the leading order, since the factor q^{-1} cancels out with σ [see Eq. (2)]. In Fig. 2 we show $\delta\Phi_{\text{GW}}^\sigma(t)$ and the spin correction to the *accumulated* GW phase, $\Phi_{\text{GW}}^{\text{tot}} = \Phi_{\text{GW}}(t_{\text{ref}})$, for some representative examples. Our results are in overall agreement with previous analyses that used “kludge” or effective-one-body waveforms [44, 77, 87], which however rely to some extent on the post-Newtonian approximation and might fail to describe accurately the contribution of small effects in the late-time EMRI dynamics. As a reference, we chose the same t_{ref} for any value of χ . In particular, we chose t_{ref} as the time to reach the ISCO for a nonspinning secondary minus 0.5 day, so that the evolution stops before the transition from inspiral to plunge (occurring near the ISCO [88, 89]) for any value of χ and \hat{a} . A useful fit of the total accumulated GW phase is:

$$\delta\Phi_{\text{GW}}^\sigma(t_{\text{ref}}) = \sum_{i=0}^3 c_i (1 - \hat{a}^2)^{i/2} + c_4 \hat{a}, \quad (9)$$

where $c_0 = 38.44$, $c_1 = -90.36$, $c_2 = 99.43$, $c_3 = -44.95$, $c_4 = 1.91$. The fit is accurate within 5% in the whole range $\hat{a} \in [0, 0.995]$, with better accuracy at large \hat{a} .

Measuring the spin of the secondary. Parameter estimation for EMRIs is a challenging problem [42, 90], especially if one wishes to use exact numerical waveforms rather than approximate ones. Here we estimate the potential to measure χ by using a simple requirement: a total dephasing ≈ 1 rad or greater is likely to substantially impact a matched-filter search, leading to a significant loss of detected events [91]. A more rigorous parameter-estimation analysis for the spin of the secondary is in progress and will appear elsewhere.

Let us consider two waveforms which differ only by the value of the spin of the secondary, χ_A and χ_B , respectively. Using Eq. (8), the minimum difference $\Delta\chi = \chi_B - \chi_A$ which would lead to a difference in phase at least of α rad is:

$$|\Delta\chi| > \frac{\alpha}{|\delta\Phi_{\text{GW}}^\sigma|}. \quad (10)$$

For a reference value $\hat{a} = 0.7$ ($\hat{a} = 0.9$) with $\alpha = 1$ [91], we obtain $|\Delta\chi| > 0.1$ ($|\Delta\chi| > 0.05$). Thus, our simplified analysis shows that EMRIs can provide a measurement of the spin of the secondary at the level of 5 – 10% for fast spinning primaries. This adds to the outstanding

accuracy in the measurements of M , \hat{a} , and μ [42, 44]. More stringent constraints would arise by an analysis of the mismatch between two waveforms [91, 92]. Requiring the latter to be smaller than $\sim 1/(2\rho^2)$, where ρ is the signal-to-noise ratio of the event, suggests using $\alpha < 1$ for back-of-the-envelope estimates [52].

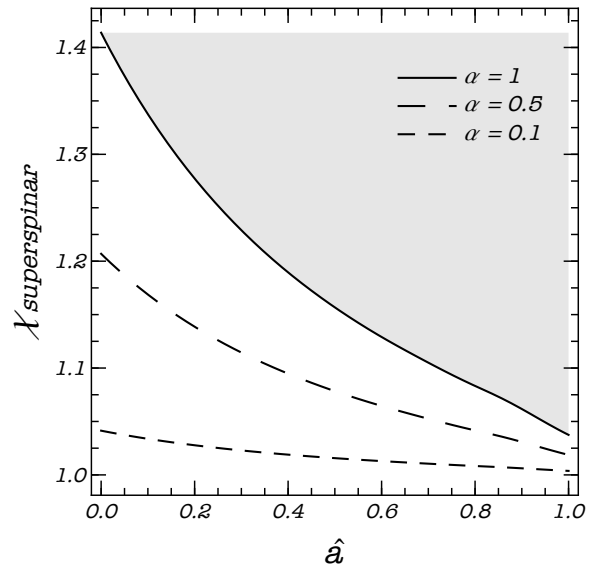


FIG. 3. Exclusion plot for the spin of a superspinar obtained using the criterion (10). A measured dephasing at the level of α rad would exclude/probe the region above each curve.

Superspinars as hints of new physics. In addition to providing an accurate and model-independent way to measure spins of stellar-mass objects [39, 44, 77, 87], EMRI detections can provide theory-agnostic tests of the Kerr bound (1) and, in particular, of superspinars [13].

As previously discussed, $\Delta\chi < 1$ for any value of \hat{a} , suggesting that the spin of a fast spinning Kerr secondary could be measured with an accuracy better than 100%. For reference values $\chi \approx \hat{a} \approx 0.7$, the accuracy is approximately 15%, which would exclude $\chi > 1$ at 3σ confidence level. Indeed, since $|\chi_A| \leq 1$ for a Kerr BH, an accuracy at the level of (say) $|\Delta\chi| > 0.1$ allows us to distinguish a Kerr BH from another fast spinning object provided the spin of the latter is $|\chi_B| \gtrsim 1 + |\Delta\chi| \approx 1.1$. In Fig. 3 we show the exclusion plot for the spin of a superspinar obtained using the criterion (10) and under the most conservative assumption, $\chi_A = 1$, as a function of the spin \hat{a} of the primary. We consider different values for the dephasing threshold α . For the standard choice of $\alpha = 1$ rad, our results suggest that it should be possible to exclude/probe the range $|\chi_B| > 1.4$ ($|\chi_B| > 1.05$) for nonspinning (highly-spinning) primaries. Since no theoretical upper bound is expected for superspinars (other, possibly, than those coming from the ergoregion instability [93–96]) a spin measurement at this level can potentially probe a vast region of the parameter space for

these objects.

One might argue that, while clearly incompatible with the secondary being a Kerr BH, a putative EMRI measurement of $\chi > 1$ could still be compatible with the secondary being a neutron star or a white dwarf. Given that neutron stars and white dwarfs have masses in the narrow range $\mu \sim (1 - 2)M_\odot$, an EMRI measurement of μ – surely available for events favorable enough to measure χ – in the range $\mu > 3M_\odot$ or $\mu \ll M_\odot$ would exclude a standard origin for the superspinner. Furthermore, even in the case in which $\mu \in (1, 2)M_\odot$, the spin of an isolated compact star is expected to be significantly smaller than the Kerr bound. As a reference, the spin of the fastest pulsar known to date is $\chi \approx 0.3$ [97]. Out of 340 observations of millisecond pulsars in the ATNF Pulsar Database [98], $\langle \chi \rangle = 0.11 \pm 0.04$, suggesting that $|\chi| > 1$ would be very unlikely². Isolated white dwarfs have comparable values of χ . The fastest spinning white dwarf to date has $\chi \approx 10$, but it is strongly accreting from a binary companion [99]. Less compact objects (such as brown dwarfs) could spin faster than the Kerr bound, but are tidally disrupted much before reaching the ISCO [39] so they can also be easily distinguishable from exotic superspinners.

Discussion. EMRIs are unique probes of fundamental physics [23, 53]. Besides offering the opportunity for exquisite tests of gravity [45–50] and of the nature of supermassive objects [42, 44, 51, 52, 100], here we have shown that they can be used to perform theory-agnostic tests of the Kerr bound. Our results suggest that EMRI detections with LISA have the potential to rule out (or detect) superspinners almost in the entire region of the parameter space. This conclusion is based on a simplistic analysis, which must be validated with a more careful study, for example including accurate waveform models, a statistical analysis that can account for correlations among the waveform parameters [87], and the fact that LISA will be a signal-driven GW detector, so that numerous simultaneously-detected sources must be suitably subtracted [40, 90, 101].

Given the fact that the secondary spin is a small effect, a faithful measurement requires having all first-order post-adiabatic effects under control. At the same time, no EMRI inspiral and post-adiabatic waveform model is complete without including the spin of the secondary along with first-order conservative and second-order dissipative self-force effects [76]. In addition to a more rigorous parameter estimation including also self-force effects and possible confusion with environmental effects

² It is also interesting to note that there is no solid explanation for the fact that the angular velocity of observed pulsars is systematically well below the theoretical (mass-shedding) limit. In this context EMRIs can provide a model-independent portal to discover neutron stars spinning faster than the current population,

(although the latter are typically negligible [102]), future work will focus on noncircular/nonequatorial orbits and on the case of misaligned spins, which introduces precession in the motion [69].

Finally, it would be very interesting to include higher multipole moments for the secondary, in particular the quadrupole moment. Although this effect is suppressed by a further $\mathcal{O}(q)$ factor and is probably too small to be detectable with LISA, it can potentially allow performing model-independent tests of the no-hair theorem on the secondary.

Acknowledgments. We thank Richard Brito and Niels Warburton for useful discussion. This work makes use of the Black Hole Perturbation Toolkit and xACT MATHEMATICA package. P.P. acknowledges financial support provided under the European Union’s H2020 ERC, Starting Grant agreement no. DarkGRA–757480, and under the MIUR PRIN and FARE programmes (GW-NEXT, CUP: B84I20000100001). The authors would like to acknowledge networking support by the COST Action CA16104 and support from the Amaldi Research Center funded by the MIUR program ”Dipartimento di Eccellenza” (CUP: B81I18001170001).

-
- [1] R. Penrose, “Asymptotic properties of fields and space-times,” *Phys. Rev. Lett.* **10** (1963) 66–68.
 - [2] R. Penrose, “Gravitational collapse and space-time singularities,” *Phys. Rev. Lett.* **14** (1965) 57–59.
 - [3] J. A. Wheeler, “Our Universe: the known and the unknown,” *The Physics Teacher* **7** (1969) 1.
 - [4] S. W. Hawking, “Black Holes and Thermodynamics,” *Phys. Rev.* **D13** (1976) 191–197.
 - [5] J. D. Bekenstein, “Black holes and the second law,” *Lett. Nuovo Cim.* **4** (1972) 737–740.
 - [6] J. D. Bekenstein, “Black holes and entropy,” *Phys. Rev.* **D7** (1973) 2333–2346.
 - [7] B. Carter, “Hamilton-Jacobi and Schrodinger separable solutions of Einstein’s equations,” *Commun. Math. Phys.* **10** no. 4, (1968) 280–310.
 - [8] B. Carter, “Global structure of the Kerr family of gravitational fields,” *Phys. Rev.* **174** (1968) 1559–1571.
 - [9] C. M. Will, “The Confrontation between General Relativity and Experiment,” *Living Rev. Rel.* **17** (2014) 4, [arXiv:1403.7377](https://arxiv.org/abs/1403.7377) [gr-qc].
 - [10] N. Yunes, K. Yagi, and F. Pretorius, “Theoretical Physics Implications of the Binary Black-Hole Mergers GW150914 and GW151226,” *Phys. Rev.* **D94** no. 8, (2016) 084002, [arXiv:1603.08955](https://arxiv.org/abs/1603.08955) [gr-qc].
 - [11] **LIGO Scientific, Virgo** Collaboration, B. P. Abbott *et al.*, “Tests of general relativity with GW150914,” *Phys. Rev. Lett.* **116** no. 22, (2016) 221101, [arXiv:1602.03841](https://arxiv.org/abs/1602.03841) [gr-qc]. [Erratum: *Phys. Rev. Lett.* **121**, no. 12, 129902 (2018)].
 - [12] We use geometric units, $G = c = 1$, and we define the Riemann tensor as $R_{\mu\nu\sigma}{}^\delta \omega_\delta = 2\nabla_{[\mu} \nabla_{\nu]} \omega_\sigma$, where ∇_μ is the covariant derivative and ω_δ an arbitrary 1-form, while the square brackets denotes the

- antisymmetrization. This is the same notation adopted in the package xCOBA of the software MATHEMATICA, which we used for all tensor computation. The metric signature is $(-, +, +, +)$.
- [13] E. G. Gimon and P. Horava, “Astrophysical violations of the Kerr bound as a possible signature of string theory,” *Phys. Lett.* **B672** (2009) 299–302, [arXiv:0706.2873 \[hep-th\]](#).
- [14] S. D. Mathur, “Fuzzballs and the information paradox: A Summary and conjectures,” [arXiv:0810.4525 \[hep-th\]](#).
- [15] S. Giusto, O. Lunin, S. D. Mathur, and D. Turton, “D1-D5-P microstates at the cap,” *JHEP* **02** (2013) 050, [arXiv:1211.0306 \[hep-th\]](#).
- [16] I. Bena, A. Puhm, and B. Vercocke, “Metastable Supertubes and non-extremal Black Hole Microstates,” *JHEP* **04** (2012) 100, [arXiv:1109.5180 \[hep-th\]](#).
- [17] I. Bena, S. Giusto, R. Russo, M. Shigemori, and N. P. Warner, “Habemus Superstratum! A constructive proof of the existence of superstrata,” *JHEP* **05** (2015) 110, [arXiv:1503.01463 \[hep-th\]](#).
- [18] M. Bianchi, D. Consoli, A. Grillo, and J. F. Morales, “The dark side of fuzzball geometries,” *JHEP* **05** (2019) 126, [arXiv:1811.02397 \[hep-th\]](#).
- [19] V. Cardoso and P. Pani, “Testing the nature of dark compact objects: a status report,” *Living Rev. Rel.* **22** no. 1, (2019) 4, [arXiv:1904.05363 \[gr-qc\]](#).
- [20] C. Bambi, “Testing the Kerr black hole hypothesis,” *Mod. Phys. Lett.* **A26** (2011) 2453–2468, [arXiv:1109.4256 \[gr-qc\]](#).
- [21] E. Berti *et al.*, “Testing General Relativity with Present and Future Astrophysical Observations,” *Class. Quant. Grav.* **32** (2015) 243001, [arXiv:1501.07274 \[gr-qc\]](#).
- [22] K. Yagi and L. C. Stein, “Black Hole Based Tests of General Relativity,” *Class. Quant. Grav.* **33** no. 5, (2016) 054001, [arXiv:1602.02413 \[gr-qc\]](#).
- [23] L. Barack *et al.*, “Black holes, gravitational waves and fundamental physics: a roadmap,” *Class. Quant. Grav.* **36** no. 14, (2019) 143001, [arXiv:1806.05195 \[gr-qc\]](#).
- [24] F. D. Ryan, “Spinning boson stars with large selfinteraction,” *Phys. Rev.* **D55** (1997) 6081–6091.
- [25] P. Pani, C. F. B. Macedo, L. C. B. Crispino, and V. Cardoso, “Slowly rotating black holes in alternative theories of gravity,” *Phys. Rev.* **D84** (2011) 087501, [arXiv:1109.3996 \[gr-qc\]](#).
- [26] B. Kleihaus, J. Kunz, and E. Radu, “Rotating Black Holes in Dilatonic Einstein-Gauss-Bonnet Theory,” *Phys. Rev. Lett.* **106** (2011) 151104, [arXiv:1101.2868 \[gr-qc\]](#).
- [27] C. A. R. Herdeiro and E. Radu, “Kerr black holes with scalar hair,” *Phys. Rev. Lett.* **112** (2014) 221101, [arXiv:1403.2757 \[gr-qc\]](#).
- [28] D. Ayzenberg and N. Yunes, “Slowly-Rotating Black Holes in Einstein-Dilaton-Gauss-Bonnet Gravity: Quadratic Order in Spin Solutions,” *Phys. Rev.* **D90** (2014) 044066, [arXiv:1405.2133 \[gr-qc\]](#). [Erratum: *Phys. Rev.* **D91**, no. 6, 069905 (2015)].
- [29] A. Maselli, P. Pani, L. Gualtieri, and V. Ferrari, “Rotating black holes in Einstein-Dilaton-Gauss-Bonnet gravity with finite coupling,” *Phys. Rev.* **D92** no. 8, (2015) 083014, [arXiv:1507.00680 \[gr-qc\]](#).
- [30] E. Barausse, T. P. Sotiriou, and I. Vega, “Slowly rotating black holes in Einstein-ther theory,” *Phys. Rev.* **D93** no. 4, (2016) 044044, [arXiv:1512.05894 \[gr-qc\]](#).
- [31] C. Herdeiro, E. Radu, and H. Rnarsson, “Kerr black holes with Proca hair,” *Class. Quant. Grav.* **33** no. 15, (2016) 154001, [arXiv:1603.02687 \[gr-qc\]](#).
- [32] P. V. P. Cunha, C. A. R. Herdeiro, and E. Radu, “Spontaneously Scalarized Kerr Black Holes in Extended Scalar-TensorGauss-Bonnet Gravity,” *Phys. Rev. Lett.* **123** no. 1, (2019) 011101, [arXiv:1904.09997 \[gr-qc\]](#).
- [33] A. Maselli, H. O. Silva, M. Minamitsuji, and E. Berti, “Slowly rotating black hole solutions in Horndeski gravity,” *Phys. Rev.* **D92** no. 10, (2015) 104049, [arXiv:1508.03044 \[gr-qc\]](#).
- [34] **LIGO Scientific, Virgo** Collaboration, B. Abbott *et al.*, “GWTC-1: A Gravitational-Wave Transient Catalog of Compact Binary Mergers Observed by LIGO and Virgo during the First and Second Observing Runs,” *Phys. Rev. X* **9** no. 3, (2019) 031040, [arXiv:1811.12907 \[astro-ph.HE\]](#).
- [35] L. Blanchet, “Gravitational radiation from post-Newtonian sources and inspiralling compact binaries,” *Living Rev. Rel.* **9** (2006) 4.
- [36] J. B. Hartle, “Tidal Friction in Slowly Rotating Black Holes,” *Phys. Rev.* **D8** (1973) 1010–1024.
- [37] S. A. Hughes, “Evolution of circular, nonequatorial orbits of kerr black holes due to gravitational-wave emission. ii. inspiral trajectories and gravitational waveforms,” *Phys. Rev. D* **64** (Aug, 2001) 064004. <https://link.aps.org/doi/10.1103/PhysRevD.64.064004>.
- [38] A. Maselli, P. Pani, V. Cardoso, T. Abdelsalhin, L. Gualtieri, and V. Ferrari, “Probing Planckian corrections at the horizon scale with LISA binaries,” *Phys. Rev. Lett.* **120** no. 8, (2018) 081101, [arXiv:1703.10612 \[gr-qc\]](#).
- [39] G. A. Piovano, A. Maselli, and P. Pani, “Extreme mass ratio inspirals with spinning secondary: a detailed study of equatorial circular motion,” [arXiv:2004.02654 \[gr-qc\]](#).
- [40] **LISA** Collaboration, P. Amaro-Seoane *et al.*, “Laser Interferometer Space Antenna,” [arXiv:1702.00786 \[astro-ph.IM\]](#).
- [41] V. Baibhav *et al.*, “Probing the Nature of Black Holes: Deep in the mHz Gravitational-Wave Sky,” [arXiv:1908.11390 \[astro-ph.HE\]](#).
- [42] S. Babak, J. Gair, A. Sesana, E. Barausse, C. F. Sopuerta, C. P. L. Berry, E. Berti, P. Amaro-Seoane, A. Petiteau, and A. Klein, “Science with the space-based interferometer LISA. V: Extreme mass-ratio inspirals,” *Phys. Rev.* **D95** no. 10, (2017) 103012, [arXiv:1703.09722 \[gr-qc\]](#).
- [43] K. Glampedakis and S. Babak, “Mapping spacetimes with LISA: Inspiral of a test-body in a ‘quasi-Kerr’ field,” *Class. Quant. Grav.* **23** (2006) 4167–4188, [arXiv:gr-qc/0510057 \[gr-qc\]](#).
- [44] L. Barack and C. Cutler, “Using LISA EMRI sources to test off-Kerr deviations in the geometry of massive black holes,” *Phys. Rev.* **D75** (2007) 042003, [arXiv:gr-qc/0612029 \[gr-qc\]](#).
- [45] C. F. Sopuerta and N. Yunes, “Extreme and Intermediate-Mass Ratio Inspirals in Dynamical Chern-Simons Modified Gravity,” *Phys. Rev.* **D80**

- (2009) 064006, [arXiv:0904.4501 \[gr-qc\]](#).
- [46] N. Yunes, P. Pani, and V. Cardoso, “Gravitational Waves from Quasicircular Extreme Mass-Ratio Inspirals as Probes of Scalar-Tensor Theories,” *Phys. Rev. D* **85** (2012) 102003, [arXiv:1112.3351 \[gr-qc\]](#).
- [47] P. Pani, V. Cardoso, and L. Gualtieri, “Gravitational waves from extreme mass-ratio inspirals in Dynamical Chern-Simons gravity,” *Phys. Rev. D* **83** (2011) 104048, [arXiv:1104.1183 \[gr-qc\]](#).
- [48] E. Barausse, N. Yunes, and K. Chamberlain, “Theory-Agnostic Constraints on Black-Hole Dipole Radiation with Multiband Gravitational-Wave Astrophysics,” *Phys. Rev. Lett.* **116** no. 24, (2016) 241104, [arXiv:1603.04075 \[gr-qc\]](#).
- [49] K. Chamberlain and N. Yunes, “Theoretical Physics Implications of Gravitational Wave Observation with Future Detectors,” *Phys. Rev. D* **96** no. 8, (2017) 084039, [arXiv:1704.08268 \[gr-qc\]](#).
- [50] V. Cardoso, G. Castro, and A. Maselli, “Gravitational waves in massive gravity theories: waveforms, fluxes and constraints from extreme-mass-ratio mergers,” *Phys. Rev. Lett.* **121** no. 25, (2018) 251103, [arXiv:1809.00673 \[gr-qc\]](#).
- [51] P. Pani and A. Maselli, “Love in Extrema Ratio,” *Int. J. Mod. Phys. D* **28** no. 14, (2019) 1944001, [arXiv:1905.03947 \[gr-qc\]](#).
- [52] S. Datta, R. Brito, S. Bose, P. Pani, and S. A. Hughes, “Tidal heating as a discriminator for horizons in extreme mass ratio inspirals,” *Phys. Rev. D* **101** no. 4, (2020) 044004, [arXiv:1910.07841 \[gr-qc\]](#).
- [53] E. Barausse *et al.*, “Prospects for Fundamental Physics with LISA,” [arXiv:2001.09793 \[gr-qc\]](#).
- [54] E. Poisson, “The Motion of point particles in curved space-time,” *Living Rev. Rel.* **7** (2004) 6, [arXiv:gr-qc/0306052 \[gr-qc\]](#).
- [55] L. Barack, “Gravitational self force in extreme mass-ratio inspirals,” *Class. Quant. Grav.* **26** (2009) 213001, [arXiv:0908.1664 \[gr-qc\]](#).
- [56] M. Mathisson, “Neue mechanik materieller systemes,” *Acta Phys. Polon.* **6** (1937) 163–2900.
- [57] A. Papapetrou, “Spinning test particles in general relativity. 1.,” *Proc. Roy. Soc. Lond.* **A209** (1951) 248–258.
- [58] E. Corinaldesi and A. Papapetrou, “Spinning test particles in general relativity. 2.,” *Proc. Roy. Soc. Lond.* **A209** (1951) 259–268.
- [59] W. Tulczyjew, “Motion of multipole particles in general relativity theory,” *Acta Phys. Pol.* **18** (1959) 393.
- [60] W. Dixon, “A covariant multipole formalism for extended test bodies in general relativity,” *Il Nuovo Cimento* **34** no. 2, (Oct, 1964) 317–339.
- [61] W. G. Dixon, “Dynamics of extended bodies in general relativity. I. Momentum and angular momentum,” *Proc. Roy. Soc. Lond.* **A314** (1970) 499–527.
- [62] W. G. Dixon, “Dynamics of extended bodies in general relativity. II. Moments of the charge-current vector,” *Proc. Roy. Soc. Lond.* **A319** (1970) 509–547.
- [63] J. Steinhoff and D. Puetzfeld, “Multipolar equations of motion for extended test bodies in General Relativity,” *Phys. Rev. D* **81** (2010) 044019, [arXiv:0909.3756 \[gr-qc\]](#).
- [64] K. Kyriian and O. Semerak, “Spinning test particles in a Kerr field,” *Mon. Not. Roy. Astron. Soc.* **382** (2007) 1922.
- [65] S. A. Teukolsky, “Rotating black holes - separable wave equations for gravitational and electromagnetic perturbations,” *Phys. Rev. Lett.* **29** (1972) 1114–1118.
- [66] S. Drasco and S. A. Hughes, “Gravitational wave snapshots of generic extreme mass ratio inspirals,” *Phys. Rev. D* **73** no. 2, (2006) 024027, [arXiv:gr-qc/0509101 \[gr-qc\]](#). [Erratum: *Phys. Rev. D* **88**,no.10,109905(2013); Erratum: *Phys. Rev. D* **90**,no.10,109905(2014)].
- [67] S. A. Hughes, “The Evolution of circular, nonequatorial orbits of Kerr black holes due to gravitational wave emission,” *Phys. Rev. D* **61** no. 8, (2000) 084004, [arXiv:gr-qc/9910091 \[gr-qc\]](#). [Erratum: *Phys. Rev. D* **63**,no.4,049902(2001); Erratum: *Phys. Rev. D* **65**,no.6,069902(2002); Erratum: *Phys. Rev. D* **67**,no.8,089901(2003); Erratum: *Phys. Rev. D* **78**,no.10,109902(2008); Erratum: *Phys. Rev. D* **90**,no.10,109904(2014)].
- [68] A. Maselli, N. Franchini, L. Gualtieri, and T. P. Sotiriou, “Detecting scalar fields with Extreme Mass Ratio Inspirals,” [arXiv:2004.11895 \[gr-qc\]](#).
- [69] T. Tanaka, Y. Mino, M. Sasaki, and M. Shibata, “Gravitational waves from a spinning particle in circular orbits around a rotating black hole,” *Phys. Rev. D* **54** (1996) 3762–3777, [arXiv:gr-qc/9602038 \[gr-qc\]](#).
- [70] L. M. Burko, “Orbital evolution of a particle around a black hole. 2. Comparison of contributions of spin orbit coupling and the selfforce,” *Phys. Rev. D* **69** (2004) 044011, [arXiv:gr-qc/0308003](#).
- [71] L. M. Burko and G. Khanna, “Self-force gravitational waveforms for extreme and intermediate mass ratio inspirals. III: Spin-orbit coupling revisited,” *Phys. Rev. D* **91** no. 10, (2015) 104017, [arXiv:1503.05097 \[gr-qc\]](#).
- [72] E. Harms, G. Lukes-Gerakopoulos, S. Bernuzzi, and A. Nagar, “Asymptotic gravitational wave fluxes from a spinning particle in circular equatorial orbits around a rotating black hole,” *Phys. Rev. D* **93** no. 4, (2016) 044015, [arXiv:1510.05548 \[gr-qc\]](#). [Addendum: *Phys. Rev. D* **100**,no.12,129901(2019)].
- [73] E. Harms, G. Lukes-Gerakopoulos, S. Bernuzzi, and A. Nagar, “Spinning test body orbiting around a Schwarzschild black hole: Circular dynamics and gravitational-wave fluxes,” *Phys. Rev. D* **94** no. 10, (2016) 104010, [arXiv:1609.00356 \[gr-qc\]](#).
- [74] G. Lukes-Gerakopoulos, E. Harms, S. Bernuzzi, and A. Nagar, “Spinning test-body orbiting around a Kerr black hole: circular dynamics and gravitational-wave fluxes,” *Phys. Rev. D* **96** no. 6, (2017) 064051, [arXiv:1707.07537 \[gr-qc\]](#).
- [75] N. Warburton, T. Osburn, and C. R. Evans, “Evolution of small-mass-ratio binaries with a spinning secondary,” *Phys. Rev. D* **96** no. 8, (2017) 084057, [arXiv:1708.03720 \[gr-qc\]](#).
- [76] S. Akcay, S. R. Dolan, C. Kavanagh, J. Moxon, N. Warburton, and B. Wardell, “Dissipation in extreme-mass ratio binaries with a spinning secondary,” [arXiv:1912.09461 \[gr-qc\]](#).
- [77] N. Yunes, A. Buonanno, S. A. Hughes, Y. Pan, E. Barausse, M. Miller, and W. Thrope, “Extreme Mass-Ratio Inspirals in the Effective-One-Body Approach: Quasi-Circular, Equatorial Orbits around a

- Spinning Black Hole,” *Phys. Rev. D* **83** (2011) 044044, [arXiv:1009.6013 \[gr-qc\]](#). [Erratum: *Phys.Rev.D* 88, 109904 (2013)].
- [78] B. Chen, G. Compere, Y. Liu, J. Long, and X. Zhang, “Spin and Quadrupole Couplings for High Spin Equatorial Intermediate Mass-ratio Coalescences,” *Class. Quant. Grav.* **36** no. 24, (2019) 245011, [arXiv:1901.05370 \[gr-qc\]](#).
- [79] A. Taracchini, A. Buonanno, S. A. Hughes, and G. Khanna, “Modeling the horizon-absorbed gravitational flux for equatorial-circular orbits in Kerr spacetime,” *Phys. Rev.* **D88** (2013) 044001, [arXiv:1305.2184 \[gr-qc\]](#). [Erratum: *Phys. Rev.D88*,no.10,109903(2013)].
- [80] S. E. Gralla, A. P. Porfyriadis, and N. Warburton, “Particle on the Innermost Stable Circular Orbit of a Rapidly Spinning Black Hole,” *Phys. Rev.* **D92** no. 6, (2015) 064029, [arXiv:1506.08496 \[gr-qc\]](#).
- [81] D. Kennefick, “Stability under radiation reaction of circular equatorial orbits around Kerr black holes,” *Phys. Rev. D* **58** (1998) 064012, [arXiv:gr-qc/9805102](#).
- [82] T. Hinderer and E. E. Flanagan, “Two timescale analysis of extreme mass ratio inspirals in Kerr. I. Orbital Motion,” *Phys. Rev.* **D78** (2008) 064028, [arXiv:0805.3337 \[gr-qc\]](#).
- [83] A. Pound, “Second-order gravitational self-force,” *Phys. Rev. Lett.* **109** (2012) 051101, [arXiv:1201.5089 \[gr-qc\]](#).
- [84] Data and relevant codes are publicly available at <https://web.uniroma1.it/gmunu>.
- [85] J. Steinhoff and D. Puetzfeld, “Influence of internal structure on the motion of test bodies in extreme mass ratio situations,” *Phys. Rev.* **D86** (2012) 044033, [arXiv:1205.3926 \[gr-qc\]](#).
- [86] P. I. Jefremov, O. Yu. Tsupko, and G. S. Bisnovatyi-Kogan, “Innermost stable circular orbits of spinning test particles in Schwarzschild and Kerr space-times,” *Phys. Rev.* **D91** no. 12, (2015) 124030, [arXiv:1503.07060 \[gr-qc\]](#).
- [87] E. Huerta and J. R. Gair, “Importance of including small body spin effects in the modelling of extreme and intermediate mass-ratio inspirals,” *Phys. Rev. D* **84** (2011) 064023, [arXiv:1105.3567 \[gr-qc\]](#).
- [88] A. Ori and K. S. Thorne, “The Transition from inspiral to plunge for a compact body in a circular equatorial orbit around a massive, spinning black hole,” *Phys. Rev. D* **62** (2000) 124022, [arXiv:gr-qc/0003032](#).
- [89] O. Burke, J. R. Gair, and J. Simn, “Transition from Inspiral to Plunge: A Complete Near-Extremal Trajectory and Associated Waveform,” *Phys. Rev. D* **101** no. 6, (2020) 064026, [arXiv:1909.12846 \[gr-qc\]](#).
- [90] A. J. K. Chua, N. Korsakova, C. J. Moore, J. R. Gair, and S. Babak, “Gaussian processes for the interpolation and marginalization of waveform error in extreme-mass-ratio-inspiral parameter estimation,” *Phys. Rev.* **D101** no. 4, (2020) 044027, [arXiv:1912.11543 \[astro-ph.IM\]](#).
- [91] L. Lindblom, B. J. Owen, and D. A. Brown, “Model Waveform Accuracy Standards for Gravitational Wave Data Analysis,” *Phys. Rev.* **D78** (2008) 124020, [arXiv:0809.3844 \[gr-qc\]](#).
- [92] E. E. Flanagan and S. A. Hughes, “Measuring gravitational waves from binary black hole coalescences: 2. The Waves’ information and its extraction, with and without templates,” *Phys. Rev.* **D57** (1998) 4566–4587, [arXiv:gr-qc/9710129 \[gr-qc\]](#).
- [93] P. Pani, E. Barausse, E. Berti, and V. Cardoso, “Gravitational instabilities of superspinars,” *Phys. Rev.* **D82** (2010) 044009, [arXiv:1006.1863 \[gr-qc\]](#).
- [94] E. Maggio, P. Pani, and V. Ferrari, “Exotic Compact Objects and How to Quench their Ergoregion Instability,” *Phys. Rev.* **D96** no. 10, (2017) 104047, [arXiv:1703.03696 \[gr-qc\]](#).
- [95] E. Maggio, V. Cardoso, S. R. Dolan, and P. Pani, “Ergoregion instability of exotic compact objects: electromagnetic and gravitational perturbations and the role of absorption,” *Phys. Rev. D* **99** no. 6, (2019) 064007, [arXiv:1807.08840 \[gr-qc\]](#).
- [96] R. Roy, P. Kocherlakota, and P. S. Joshi, “Mode stability of a near-extremal Kerr superspinner,” [arXiv:1911.06169 \[gr-qc\]](#).
- [97] J. W. Hessels, S. M. Ransom, I. H. Stairs, P. C. C. Freire, V. M. Kaspi, and F. Camilo, “A radio pulsar spinning at 716-hz,” *Science* **311** (2006) 1901–1904, [arXiv:astro-ph/0601337](#).
- [98] R. N. Manchester, G. B. Hobbs, A. Teoh, and M. Hobbs, “The Australia Telescope National Facility pulsar catalogue,” *Astron. J.* **129** (2005) 1993, [arXiv:astro-ph/0412641](#).
- [99] B. C. Bisscheroux, O. R. Pols, P. Kahabka, T. Belloni, and E. P. J. van den Heuvel, “The nature of the bright subdwarf HD 49798 and its X-ray pulsating companion.,” *A&A* **317** (Feb., 1997) 815–822.
- [100] P. Pani, E. Berti, V. Cardoso, Y. Chen, and R. Norte, “Gravitational-wave signatures of the absence of an event horizon. II. Extreme mass ratio inspirals in the spacetime of a thin-shell gravastar,” *Phys. Rev.* **D81** (2010) 084011, [arXiv:1001.3031 \[gr-qc\]](#).
- [101] LISA Data Challenge Working Group. LISA Data Challenges, 2019. <https://lisa-ldc.lal.in2p3.fr>.
- [102] E. Barausse, V. Cardoso, and P. Pani, “Can environmental effects spoil precision gravitational-wave astrophysics?,” *Phys. Rev. D* **89** no. 10, (2014) 104059, [arXiv:1404.7149 \[gr-qc\]](#).